sci
where science meets business
www.soci.org

Mini Review

Understanding surfaces and buried interfaces of polymer materials at the molecular level using sum frequency generation vibrational spectroscopy

Zhan Chen*

Department of Chemistry, Department of Macromolecular Science and Engineering, Applied Physics Program, and Optical Physics Interdisciplinary Laboratory, University of Michigan, Ann Arbor, MI 48109, USA

Abstract: This paper reviews recent progress in the studies on polymer surfaces/interfaces using sum frequency generation (SFG) vibrational spectroscopy. SFG theory, technique, and some experimental details have been presented. The review is focused on the SFG studies on buried interfaces involving polymer materials, such as polymer–water interfaces and polymer–polymer interfaces. Molecular interactions between polymer surfaces and adhesion promoters as well as biological molecules such as proteins and peptides have also been elucidated using SFG. This review demonstrates that SFG is a powerful technique to characterize molecular level structural information of complicated polymer surfaces and interfaces *in situ*.
© 2006 Society of Chemical Industry

Keywords: sum frequency generation; vibrational spectroscopy; polymer surfaces and interfaces; polymer biocompatibility; polymer adhesion

INTRODUCTION

Polymer materials are widely used everywhere, ranging from high-tech industry to everyday life. Polymer surface properties play important roles in many of these applications such as biomedical materials, marine anti-biofouling coatings, microelectronic devices, and substrates for growing drugs.[1–5] Polymer surface properties are determined by molecular surface structures. To develop polymer surfaces with desired properties, it is crucial to manipulate accurately polymer surface structures. The first step for rational design of polymer surfaces is to develop techniques to characterize polymer surface structures at the molecular level. Only after the development of such techniques can polymer surface structures be characterized in detail; detailed correlations between polymer surface structures and properties can then be established, aiding in the development of polymer surfaces with designed properties. In the last few decades, a variety of surface-sensitive techniques have been developed. However, most such techniques require a high vacuum to operate, or cannot probe molecular level surface structure, or lack desired surface specificity. Probing polymer surface structures at the molecular level *in situ* in real time is still not easy.

Recently sum frequency generation (SFG) vibrational spectroscopy has been developed into a powerful and unique technique to investigate surface structures of various polymer materials, including pure polymers, polymer blends, and copolymers.[6] In addition to the surface studies in air, buried interfaces such as polymer surfaces in water, polymer–polymer interfaces, and polymer–inorganic solid interfaces have also been examined using SFG.[6] Furthermore, SFG has been used to investigate molecular interactions between polymer surfaces and biological molecules such as proteins and peptides to understand polymer biocompatibility, and interactions between polymers and adhesion promoters to understand molecular mechanisms of polymer adhesion.[7–9] Usually, to analyze buried interfaces (e.g. polymer–polymer interfaces) using conventional surface-sensitive techniques, it is necessary to break such interfaces and expose the two resulting surfaces to air for study. After the interface is broken, much structural information may be lost and the detected results from the two resulting surfaces may not represent the originally buried interface structures.

* Correspondence to: Zhan Chen, Department of Chemistry, Department of Macromolecular Science and Engineering, Applied Physics Program, and Optical Physics Interdisciplinary Laboratory, University of Michigan, Ann Arbor, MI 48109, USA
E-mail: zhanc@umich.edu
Contract/grant sponsor: NSF; contract/grant number: CHE-0315857; CHE-0449469
Contract/grant sponsor: ONR; contract/grant number: N00014-02-1-0832
Contract/grant sponsor: Beckman Foundation
Contract/grant sponsor: Dow Corning Corporation
(*Received 25 May 2006; revised version received 31 July 2006; accepted 17 October 2006*)
Published online 29 December 2006; DOI: 10.1002/pi.2201

© 2006 Society of Chemical Industry. *Polym Int* 0959–8103/2006/$30.00

WILEY InterScience® DISCOVER SOMETHING GREAT

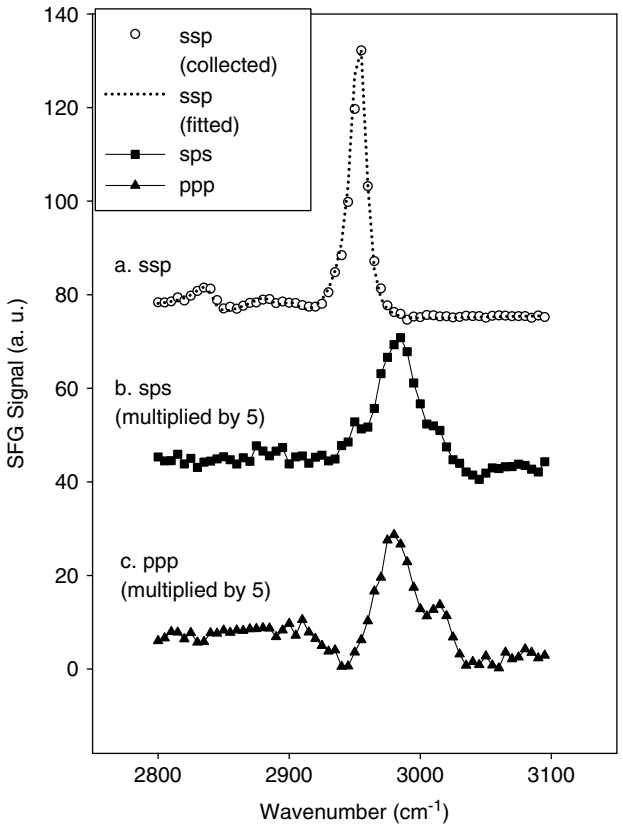

Figure 1. SFG spectra collected from PMMA surface in air with different polarization combinations of input and output laser beams: (a) ssp (s, polarized SFG signal; s, polarized visible input; p, polarized IR input); (b) sps; (c) ppp. (Reproduced with permission from *J Phys Chem B* **105**:12118–12125 (2001). Copyright 2001 American Chemical Society).

However, SFG can detect *in situ* structural information of buried interfaces, providing direct observation.

SFG VIBRATIONAL SPECTROSCOPY

SFG is a second-order nonlinear optical spectroscopic technique, which provides vibrational spectra of surfaces and interfaces.[10–13] Vibrational spectra are fingerprints of molecules; therefore, SFG can elucidate surface/interface structures at the molecular level. An SFG spectrum looks like a Fourier transform infrared (FTIR) or Raman spectrum, which plots the signal intensity as a function of IR wavenumber (Fig. 1); however, the mechanism of SFG is different. FTIR is an absorption spectroscopy: when an IR photon hits a molecule, if its frequency matches a resonance of a vibrational mode of the molecule, it may be absorbed. In addition to the frequency resonance, whether a vibrational mode is IR active or not is determined by the IR selection rule, which is controlled by the dipole moment change during the vibration. A normal Raman process is a scattering process which involves two photons. An incoming photon interacts with a molecule and the energy of the outgoing photon is modulated by a vibrational motion of the molecule if a Raman process occurs. The incoming photon can gain or lose energy from or to the molecule. The energy difference between the two photons matches the energy difference between vibrational states of the molecule. That is to say, the output photon can only carry certain amounts of energy. In addition to such energy conservation, whether a vibrational mode is Raman active or not is controlled by the polarizability change during the vibration.

Unlike FTIR (one photon) and Raman (two photons), an SFG process involves three photons: two incoming photons and one outgoing photon. The outgoing photon carries the sum frequency (or sum energy) of the two input photons. In a typical SFG experiment using a frequency scanning system, two input beams, a visible light and a frequency tunable infrared light, shine on a surface/interface (Fig. 2(a)). As a result, there are two natural reflected beams from the surface/interface: one is infrared and the other is visible. These two reflected beams would not be collected in an SFG experiment. A third reflection, which has the sum frequency of the two incoming beams, is detected. The intensity of the third reflection beam (sum frequency signal beam) is collected and plotted as a function of the input IR wavenumber, generating an SFG spectrum. When the frequency of the input infrared beam matches a vibrational resonance of molecules on the surface/interface, the SFG signal is enhanced. Figure 2(b) shows the energy level diagrams of the IR, Raman, and SFG processes. Clearly an SFG process is a combination of an IR

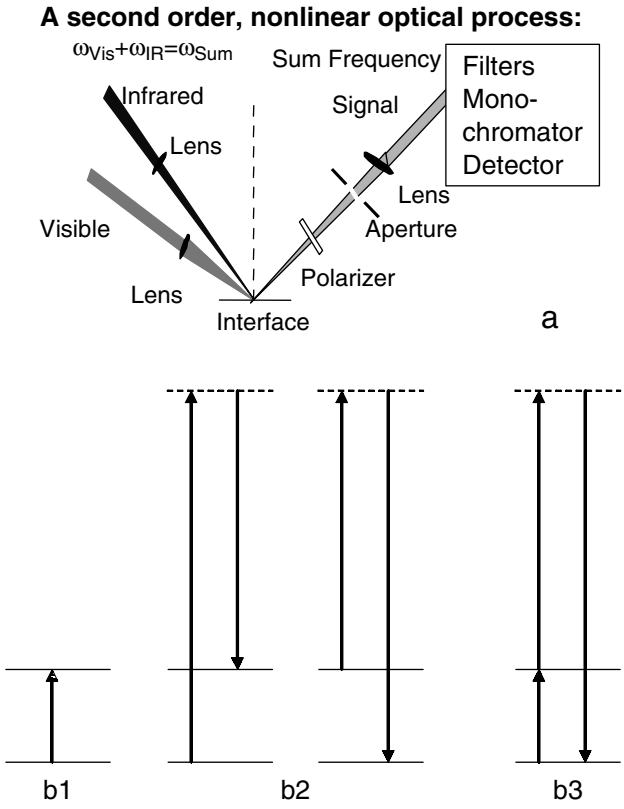

Figure 2. (a) SFG experimental geometry. Two input beams are overlapped on the sample surface/interface; sum frequency signal is collected. (b) Energy level diagrams for: (1) IR absorption; (2) Stokes (left) and anti-Stokes (right) Raman scattering; (3) SFG.

Polym Int **56**:577–587 (2007)
DOI: 10.1002/pi

process and anti-Stokes Raman scattering. Only the vibrational modes that are both IR and Raman active can be observed in SFG experiments.

Usually the SFG signal is only produced by the surface/interface molecules because of the SFG selection rule. Under the electric dipole approximation, SFG signal intensity is proportional to the square of a property, second-order nonlinear susceptibility $\chi^{(2)}$, of the material. This $\chi^{(2)}$ is a polar tensor, which means that it will change sign under the inversion operation: $\chi^{(2)}(r) = -\chi^{(2)}(-r)$. However, for any material with inversion symmetry, nothing will be changed under the inversion operation: $\chi^{(2)}(r) = \chi^{(2)}(-r)$. Clearly the only possible solution for the above two equations is $\chi^{(2)} = 0$. Therefore for materials with inversion symmetry no SFG signal is detected (under the dipole approximation). Most bulk polymer materials such as polymer melts and most solid polymer systems generally do have inversion symmetry, because various functional groups in the bulk of such polymers more or less have a random orientation distribution; thus these bulk materials would not generate SFG signals. However, for molecules or functional groups on surfaces/interfaces, because inversion symmetry is broken at the surface/interface, the equation $\chi^{(2)}(r) = \chi^{(2)}(-r)$ is no longer valid. Here, $\chi^{(2)}$ does not need to be zero, and SFG signals can be detected from such moieties on surfaces/interfaces. Due to this selection rule, SFG is intrinsically surface/interface sensitive, with submonolayer surface sensitivity. Excellent research has been done using attenuated total reflection (ATR)-FTIR and surface-enhanced Raman scattering (SERS) to study polymer surfaces. The surface sensitivity of ATR-FTIR is limited by the penetration depth of the IR light, which is of the order of hundreds of nanometers or a few micrometers. Thus its surface sensitivity is not comparable to SFG. SERS requires a metal substrate, and is not as flexible as SFG, which can be used to study many surfaces and interfaces where the inversion symmetry is broken.

Due to the weak SFG signals, usually picosecond or femtosecond pulsed lasers are used to generate incident laser beams for SFG experiments. Two different kinds of systems, including a broad-band system and a frequency scanning system, are typically used in SFG research in various research groups.[14] Frequency scanning systems are used in the author's laboratory, and more details regarding the broad-band system can be found in the literature[14] and are not discussed here. The SFG setups in the author's laboratory have been described in detail in previous publications.[15–19] They are composed of four components each: a picosecond Nd:YAG laser, a harmonic unit with two KD*P crystals, an optical parametric generation (OPG)/optical parametric amplification (OPA) and difference frequency generation (DFG) system based on LBO and $AgGaS_2$ crystals, and a detection system containing two channels: the signal channel and the reference channel. The visible beam (532 nm) is generated by frequency-doubling the fundamental output pulses of 20 ps pulsewidth from the Nd:YAG laser. The IR beam can be tuned from 1000 to 4300 cm^{-1}, generated from the OPG/OPA and DFG system. A new DFG system using a GaSe crystal to extend IR tunability to 650 cm^{-1} was also installed. The incident angles of the visible and the IR input beams can be varied. In a standard experiment, they are 60° and 55° *versus* the surface normal, respectively. The diameters of both visible and IR beams at the surface are about 500 μm. The SFG signal from the surface is collected by a photomultiplier and processed with a gated integrator. Two photodiodes are used to monitor the input visible beam and IR beam powers by collecting the back reflections of these two beams from focus lenses. Usually the pulse energies of the IR and visible beams are around 100 and 200 μJ, respectively. SFG spectra collected from the sample surfaces can be normalized by the power of the input laser beams. SFG spectra with different polarization combinations such as ssp (s, polarized output; s, polarized visible input; and p, polarized IR input), ppp, and sps can be collected.

In most cases SFG spectra are collected from optically flat surfaces. Most SFG studies have focused on the C–H, N–H, or O–H stretching frequency regions, because such signals are relatively easier to detect and their data analysis has been extensively studied. In our experiments, a typical spectrum in the C–H stretching region can be collected within several minutes. SFG signals in other spectral regions, such as SFG amide I signals from interfacial proteins, SFG C–F stretching signals, and SFG SO_3 signals have been reported and analyzed.[20–22] Therefore, currently SFG signals in a variety of spectral regions can be observed and studied.

The SFG output intensity in the reflected direction can be written as[6]

$$I(\omega) = \frac{8\pi^3\omega^2 \sec^2\beta}{c^3 n(\omega)n(\omega_1)n(\omega_2)} |\chi^{(2)}_{\text{eff}}|^2 I_1(\omega_1) I_2(\omega_2) \qquad (1)$$

where $n(\omega)$ is the refractive index of the medium at frequency ω, β is the reflection angle of the sum frequency field, $I_1(\omega_1)$ and $I_2(\omega_2)$ are the intensities of the two input fields, and $\chi^{(2)}_{\text{eff}}$ is the effective second-order nonlinear susceptibility tensor of the surface, which is proportional to the concentration of the surface functional groups. If the IR frequency (ω_2) is near vibrational resonances, we can write[6]

$$\chi^{(2)}_{\text{eff}} = \chi_{\text{nr}} + \sum_q \frac{A_q}{\omega_2 - \omega_q + i\Gamma_q} \qquad (2)$$

where χ_{nr} arises from the nonresonant background contribution, and A_q, ω_q, and Γ_q are the strength, resonant frequency, and damping coefficient of the qth vibrational mode. Values for these parameters can be deduced from fitting of the observed SFG spectra using Eqns (1) and (2). Due to the interferences between nonresonant and resonant contributions, or between different resonant modes, resonant peaks in

the SFG spectra may appear asymmetric. For most polymer materials covered in this review, however, the nonresonant contribution is small, making the spectra less complex. One example of an SFG fitted spectrum is shown in Fig. 1(a).

SFG spectra can show what kinds of molecules/functional groups are present on the surface/interface according to the peak centers of various vibrational bands in the SFG spectra. In addition, orientation information of these surface molecules/functional groups can be deduced from SFG spectra collected using different polarization combinations such as ssp, ppp, and sps. This is one of the most important reasons why it is necessary to collect SFG spectra using different polarization combinations of the input and output laser beams. According to the intensity ratio of different vibrational modes of a functional group in the same spectrum, or more frequently intensity ratio of the same peak in SFG spectra collected using different polarizations, we can deduce the orientation of the functional groups on the surface. Details regarding the quantitative analysis can be found in our previous publications[15–19] as well as references cited in such publications and are not repeated here. Several examples are discussed below to demonstrate that SFG is a unique and powerful technique to elucidate polymer surface/interface structures. The purpose of this paper is to introduce the SFG technique and its applications to the polymer research community. Therefore only a few examples will be presented instead of reviewing or summarizing all the published results of SFG studies of polymer surfaces. SFG has been applied to study molecular surface structures of various widely used polymer materials in air. Examples of these polymers include polyethylene, polypropylene, polystyrene (PS), poly(methyl methacrylate) (PMMA), polyimides, poly(ethylene glycol) (PEG), and polytetrafluoroethylene (PTFE).[15,22–29] SFG has also been used to investigate surface structures of various polymer blends in air.[30–34] In addition, surface structural changes of polymer materials induced by various surface modification methods such as UV irradiation, plasma treatment, rubbing, wet treatment, and oxygen ion and radical irradiation have been studied using SFG.[28,35–38] Such results are not summarized in this article. In the following, SFG research on polymer surfaces in water, buried polymer–solid interfaces, and interactions between polymer surfaces and biological molecules as well as adhesion promoters is presented.

EXAMPLE APPLICATIONS OF SFG TO STUDY POLYMER SURFACES AND INTERFACES

Polymer surfaces in water

Polymer materials are frequently used in an aqueous environment. Examples include biomedical polymer implants, polymer coatings for biosensors, and marine anti-biofouling coatings. To understand polymer surface structures in these real applications, it is necessary to examine polymer–water interfaces. Water contact angle experiments have been used to monitor surface structural changes of polymers after contact with water,[39] but they do not provide molecular structural information of such changes. Freeze-drying X-ray photoelectron spectroscopy (XPS) has been used, but its sample preparation is complicated and it cannot provide orientation information of functional groups on the surface.[40] The first application of SFG to study polymer surfaces in water was to monitor the surface structure of a biomedical polyurethane with silicone polydimethylsiloxane (PDMS) end groups in water.[41] The longer the polymer contacted water, the stronger is the SFG signal of the methylene symmetric stretching of urethane segments at 2851 cm^{-1}. At the same time, SFG signals from the symmetric methyl stretching of $Si-CH_3$ groups in PDMS at 2919 cm^{-1} decrease. The results indicate that the hydrophilic polyurethane groups tend to segregate more to the surface in water while the hydrophobic PDMS groups retreat to the bulk.

We have systematically investigated surface structural changes of polymethacrylates with different side chains in water.[16] No substantial structural changes of the PMMA surface in water compared to air were found. Figure 1 shows SFG spectra collected from the PMMA surface in air using different polarization combinations of the input and output beams. The ssp spectrum is dominated by the 2955 cm^{-1} peak, which is mainly contributed by the symmetric stretching mode of the ester methyl group in PMMA. Both ppp and sps spectra are dominated by two asymmetric stretching modes of the ester methyl group at 2990 and 3016 cm^{-1}, respectively. According to the intensity ratio of the symmetric stretching peak *versus* the asymmetric stretching peak in the same spectrum, or the intensity ratio of the same peak in spectra collected using different polarizations, we can deduce the orientation of the ester methyl groups on the surface.[15] It was found that the PMMA surface in air is dominated by the ester methyl groups and such ester methyl

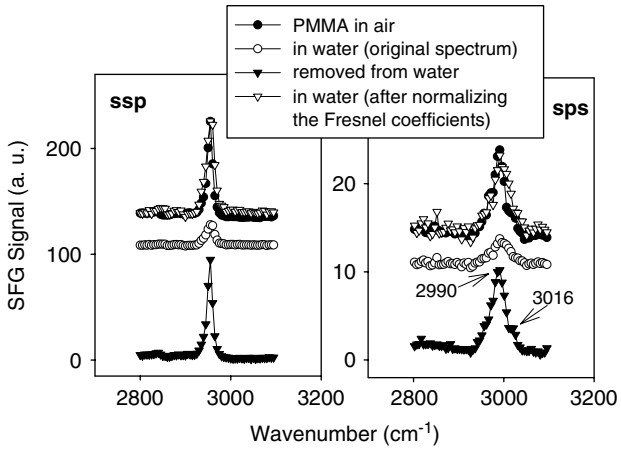

Figure 3. SFG spectra of PMMA before, during, and after contacting water. Left: ssp; right: sps. (Reproduced with permission from *J Am Chem Soc* **123**:9470–9471 (2001). Copyright 2001 American Chemical Society).

Polym Int **56**:577–587 (2007)
DOI: 10.1002/pi

groups orient more or less normally towards the surface. Figure 3 shows the ssp and sps SFG spectra collected from the PMMA–water interface *in situ*. For comparison purpose, SFG spectra collected in air and after removing the sample from water and exposing to air again are also shown in the same figure. Both ssp and sps SFG spectra of PMMA in water are dominated by the signals from ester methyl groups, similar to those of the PMMA–air interface, although they are much weaker. Detailed analysis of the spectra shows that the weaker spectra are mainly due to the changes of the Fresnel coefficients for the two interfaces because of the refractive index difference in air and water.[16] If we normalize such coefficients, SFG spectra collected in water overlap with those in air quite well (Fig. 3), showing that there is little structural change for the PMMA surface after contacting water. The spectra collected after removing the PMMA surface from water and exposing to air again are the same as those collected from the PMMA surface in air before contacting water.

Figure 4 shows ssp and sps SFG spectra collected from poly(*n*-butyl methacrylate) (PBMA)–air and PBMA–water interfaces. In air, the ssp spectrum is dominated by the symmetric stretching (2875 cm^{-1}) and Fermi resonance (2940 cm^{-1}) of methyl end group of the ester side chain, while the sps spectrum collected in air and both SFG spectra collected in water are dominated by the asymmetric stretching of the end methyl group at 2960 cm^{-1}. These results indicate that the PBMA surface is dominated by the end methyl groups of the side chain in both air and water. The orientation of such end methyl groups changes when the surface is exposed to water, shown by different intensity ratios of the symmetric/asymmetric peaks in the same spectrum or those of the same peak in different polarized spectra for the air and water cases. Such a surface change is reversible, because the SFG spectra collected from the PBMA after removing the surface from water and exposing to air again are the same as those collected in air before contacting water. This shows that the surface structure recovers after removing the PBMA sample from water and exposing it to air again. More quantitative studies on the orientation changes of the end methyl groups on the PBMA surface in water are discussed below. The poly(*n*-octyl methacrylate) (POMA) surface exhibits more substantial changes involving backbone restructuring in water, and such changes are irreversible upon removal from water, because SFG spectra cannot recover.[16] For molecules with even longer side chains, like poly(*n*-octadecyl methacrylate) (PODMA), both the surfaces in air and in water are dominated by side chains with both methyl and methylene SFG signals detected. The side-chain orientations on the PODMA surface are different in air and water, and the change in water from air is reversible.

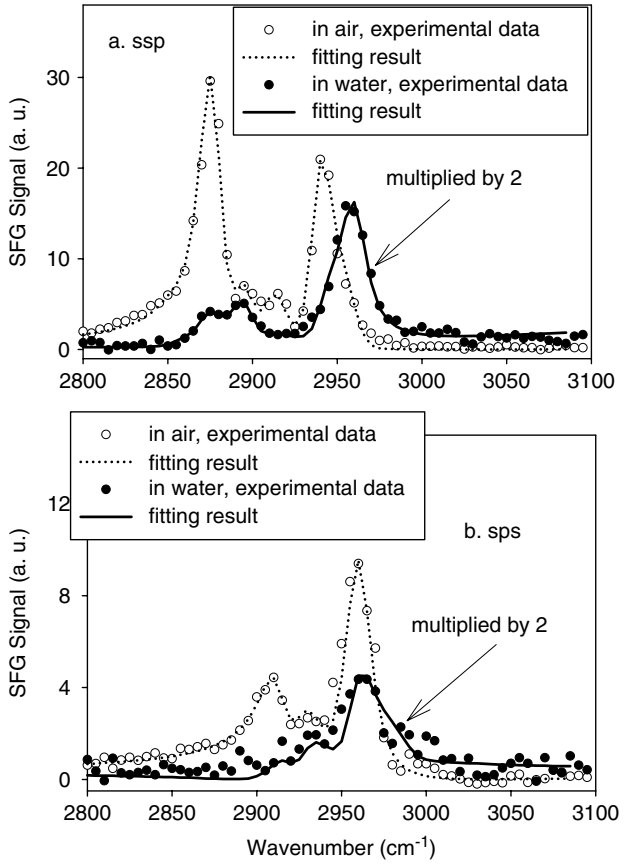

Figure 4. SFG spectra of PBMA in air and water: (a) ssp; (b) sps polarization combinations. (Reproduced with permission from *J Am Chem Soc* **124**:7016–7023 (2002). Copyright 2002 American Chemical Society).

PMMA has a very high glass transition temperature, showing that PMMA materials (perhaps also the surface molecules) are rigid. Additionally, the surface is dominated by ester methyl groups, which are more hydrophilic than regular methyl groups. When ester methyl groups interact with water, they do not need to change their orientation. Therefore the PMMA surface did not exhibit substantial structural changes in water. The surface-dominating groups on the PBMA surface in air and in water are regular methyl groups. Unfavorable interactions between these methyl groups and water drive them to orient more towards the surface, and such a surface change is reversible. The POMA glass transition temperature is very low; thus POMA molecules (including molecules on the surface) are very mobile, exhibiting a more striking and irreversible structural change in water. For PODMA, because the side chain is very long, it behaves like a long-chain hydrocarbon, resulting in a different surface restructuring behavior in water from POMA. In addition to varying the side-chain lengths, we also studied surface structural changes in water of two polymers with similar side chains but slightly different backbones: poly(ethyl methacrylate) (PEMA) and poly(ethyl acrylate) (PEA). The reversible surface restructuring behavior of PEMA in water is similar to that of PBMA: the surface-dominating end methyl groups change orientation. PEA surface exhibits an irreversible restructuring behavior similar to POMA.[42]

Polymer molecules are large molecules and thus polymer surfaces can be quite complicated. The SFG data analysis discussed above is more or less qualitative. We hope quantitatively to characterize polymer surface structures in air and in water. Our SFG studies show that a polymer surface is usually dominated by one or only a few functional groups. If we can deduce what functional groups dominate the polymer surface and determine the orientation distribution of these groups, we can more or less quantify the polymer surface structure. We want to emphasize that we need to determine orientation distribution rather than orientation angle because the same type of functional groups on a polymer surface do not necessarily adopt exactly the same orientation angle; instead, they will have an orientation distribution. For many previous SFG studies, it was assumed that all the same functional groups on a surface adopt the same orientation. By using the SFG intensity ratio (unfortunately for many functional groups the measured intensity ratios with different pairs of polarization combinations, e.g. ssp *versus* ppp and ppp *versus* sps, are dependent on each other), only one measurement can be performed, from which such an orientation of the functional groups can be deduced. We successfully combined two measurements by including SFG intensity ratio and absolute intensity measurements to deduce two parameters (average orientation and orientation distribution width) of the orientation distribution of surface-dominating methyl groups on the PBMA surface in air and in water (Fig. 5).[17] From such a study, we can say in quantitative terms that the methyl groups orient more normally towards the surface in air with a broader distribution. They tilt more towards the surface in water with a narrower distribution.

In addition to these polymethacrylates, surface restructuring of another polymethacrylate, cross-linked poly(2-hydroxyethyl methacrylate) (PHEMA), a widely used contact lens material (hydrogel), has been studied using SFG.[43] SFG measurements

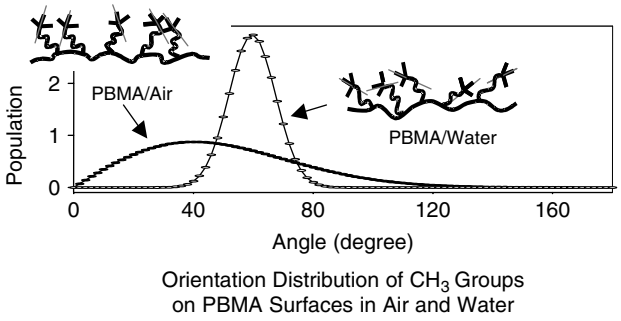

Figure 5. Orientation distribution of methyl groups on the PBMA surface in air and in water. The angle of the *x*-axis is the angle between the methyl principal axis and the surface normal. In air, the methyl groups have a small average angle, showing that they tend to stand up on the surface with a broader distribution. In water, they tend to lie down with a narrower distribution. (Reproduced with permission from *J Am Chem Soc* **124**:7016–7023 (2002). Copyright 2002 American Chemical Society).

demonstrate that PHEMA can adopt two discrete surface states depending on the environment. When PHEMA is exposed to air, polar side chains turn into the bulk, leaving the nonpolar methyl groups to project out of the surface to form a 'hydrophobic conformation'. In water, polar ethylene glycol groups migrate to the surface and coexist with methyl groups at the surface, creating a 'hydrophilic conformation'. Besides SFG studies of C–H groups of polymer surfaces in water, SFG research on C=O groups has been conducted by the Ye group and our group, indicating that hydrogen bonds can be formed between polymers and water molecules.[42,44] The Ye group showed that after biocompatible poly-(2-methoxyethyl acrylate) (PMEA) surface contacted water, its SFG C=O stretching signal had a red shift of 18 cm^{-1}, due to hydrogen bond formation.[44] Other than polymethacrylates and polyacrylates, surface structures of various PDMS materials, which are widely used as biomedical polymer implants and anti-biofouling coatings, have been investigated using SFG.[18] SFG studies of polymer surfaces in water indicate that it is feasible quantitatively to examine polymer surface structures in air and in water.

To understand how polymer surfaces respond to different chemical environments, SFG has also been applied to study surface structures of polymer materials in other liquids. For example, Richter and co-workers have studied surface structures of PS while contacting various liquids, including water, methanol, ethanol, glycerol, and hexane.[45] Qualitatively, they showed that in low-surface-tension liquids, surface-dominating phenyl groups adopt similar orientation as that in air. In high-surface-tension liquids, things are different. Quantitative orientational information of phenyl groups on the PS surface in various liquid environments has also been deduced in this work.

Buried polymer–solid interfaces

Understanding interface structures between a polymer material and a solid (which can be another polymer material) is crucial to evaluate miscibility and bulk properties of polymer blends, and adhesion at polymer–solid interfaces. The first SFG study of solid–solid interfaces involving polymer materials was the examination of the PS–sapphire interface with a total internal reflection geometry.[26] By carefully choosing the incident angles of the input beams, the PS conformation at the PS–air surface and the buried PS–sapphire interface can be explored separately. It was shown that phenyl groups tend to stand up at the PS–air interface, and tend to lie down at the PS–sapphire interface. SFG was also applied to investigate molecular structures of poly(*n*-alkyl acrylate)–sapphire interfaces as a function of temperature.[46] Upon heating, SFG spectral intensity decreases and one sharp transition close to the bulk melting temperature was observed, showing that the interfacial melting occurs at the same bulk melting temperature.

DOI: 10.1002/pi

A different method was developed using SFG to detect the buried PS–spin-on-glass (SOG) interface by spin coating a thin layer of SOG on a gold film. A PS film was then spin coated on top of the SOG surface.[47] Instead of varying the incident beam angles using the total reflection geometry as stated before, the SOG thickness was altered to generate different interference patterns of the signals generated from the two interfaces so that the PS–air interface or the buried PS–SOG interface can be probed separately. The experimental results indicated that the phenyl groups at the buried interface point away from the PS film toward the SOG–Au substrate, with an almost identical orientational distribution to that of the PS–air interface. In addition, the hydrophobic SOG surface was modified by UV-ozone to create a hydrophilic SOG surface. SFG studies on the PS–hydrophilic SOG interface show that the interface has a different structure from the PS–unmodified hydrophobic SOG interface.[48] Such structural differences can be correlated to the different adhesion properties of the two interfaces.

In our study, SFG spectra were collected with two input laser beams traveling through the substrate and the thin PS film to the PS–PBMA interface (Fig. 6). We ensured that the spectra we collected were contributed from the polymer–polymer interface, not from the PS–substrate or PBMA–air interfaces.[19] From SFG intensity ratio measurements, we found that the intensity ratio of the asymmetric stretching mode of the side-chain methyl groups of PBMA in the SFG spectra collected using different polarization combinations from the buried PBMA–PS interface is between the values of the PBMA–air and PBMA–water interfaces, indicating that the orientation of side-chain methyl groups at the buried PBMA–PS interface is between those at the PBMA–air and PBMA–water interfaces. On the PBMA surface in air, the methyl groups have greater freedom and they tend to extend into the air, leading to a small average orientation angle *versus* the surface normal. Upon contacting water, the strong repulsion between the methyl groups and water molecules directs the methyl groups away from the surface normal, resulting in a larger average orientation angle. At the PBMA–PS interface, the methyl groups interact with the phenyl groups of PS, and the repulsion must be weaker compared to that with water. The repulsion force also directs the phenyl groups away from the interface normal compared to the PS–air interface, shown by different aromatic C–H signals at the PS–PBMA and PS–air interfaces. The structure and molecular interaction at the PBMA–air, PBMA–water, and PBMA–PS interfaces would be a good project for theoretical simulation, which should be done in the future. SFG results can provide direct evidence to test such simulations.

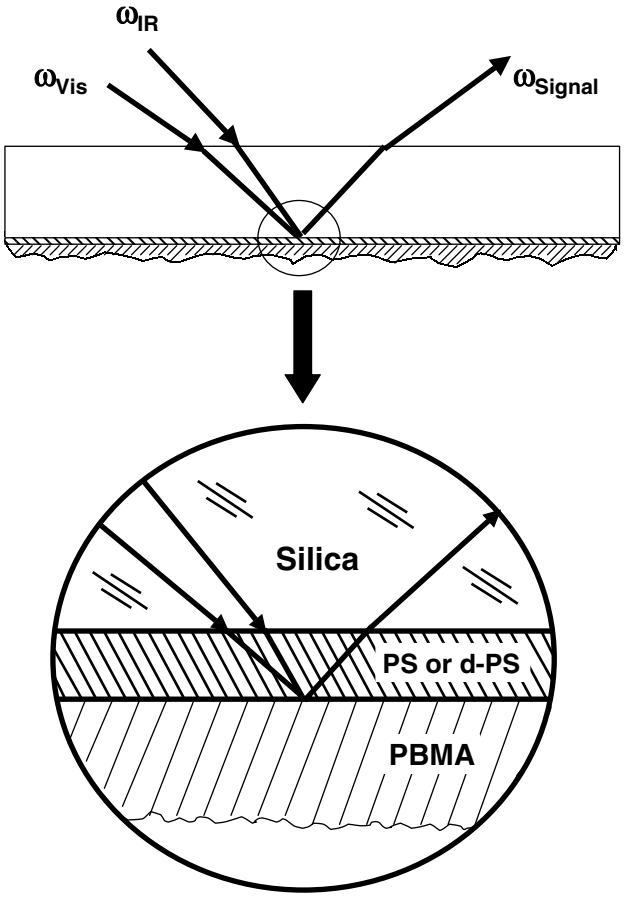

Figure 6. PBMA–PS sample for buried polymer–polymer interface study. (Reproduced with permission from *Macromolecules* **35**:8093–8097 (2003). Copyright 2003 American Chemical Society).

The Somorjai group investigated structures of PMMA and PBMA at a polymer–sapphire interface under compression using SFG.[49] Ye and colleagues studied structures of PMEA at polymer–air and polymer–PS interfaces. They found that PEMA OCH_3 groups adopt the same vector orientation.[50] The research summarized above demonstrates the feasibility and power to use SFG to probe buried interfaces involving polymer materials *in situ*.

In addition to the solid–solid interfaces, we studied interfaces between liquid polymers such as poly(ethylene glycol) (PEG) or poly(propylene glycol) (PPG) and solid materials like fused silica, PMMA, and PS. Different conformations of liquid polymers at various interfaces were observed, depending on the varied molecular interactions at the interfaces.[51,52] Since PEG and PPG are widely used as polymer surfactants, this research helps understand the interfacial activities of polymer surfactants.

Interactions between polymers and biomolecules as well as adhesion promoters

Understanding polymer–biomolecule (such as protein) interactions is important for many applications. For example, the first body reaction to a biomedical polymeric implant is protein adsorption. The adsorbed protein structures determine subsequent body reactions such as cell adhesion, controlling whether blood coagulation or an unfavorable immune response would occur and whether the implant can ultimately be

accepted by the body. The first step for marine biofouling to occur is the interaction between adhesive proteins generated by marine organisms such as mussels or barnacles and coatings of marine ships. The interactions between polymer surfaces and proteins also mediate biosensor performance, and protein separations in many systems such as micro-fluidics. We studied molecular interactions between polymers and proteins from two aspects: protein structural change at the interface and polymer surface structural change during the interactions.

We investigated protein structural information at polymer–protein solution interfaces *in situ* using SFG in both the C–H stretching and amide I frequency regions. SFG studies of C–H stretching provide structural information of protein hydrophobic side chains at interfaces,[53–57] while SFG amide I investigations reveal secondary structural or conformational information regarding interfacial proteins.[20,58–62] SFG studies showed that the same protein molecules exhibit various structures after contacting different polymers, and different time-dependent structural changes of adsorbed proteins can be observed. Fibrinogen is a good example, which shows such different time-dependent structural changes on various surfaces. The top structure in Fig. 7(a) shows a native structure of fibrinogen, which has a more or less symmetric structure with inversion symmetry. If fibrinogen adopts the same structure after being adsorbed to a surface, negligible SFG amide I signals should be observed. However, a very strong SFG signal has been detected after fibrinogen adsorbed to several surfaces such as a polyurethane (Tecoflex) surface, a polyurethane–silicone copolymer (carbosil) surface, and a fluorinated polymer surface (Fig. 8).[60] Such SFG amide I signals are centered at 1650 cm^{-1}, indicating that they mainly result from α-helical coiled coils in fibrinogen. The strong SFG amide I signals show that fibrinogen adopts a bent structure after adsorption onto these polymer surfaces (middle and lower structures in Fig. 7(a)). Different time-dependent changes of such a bent structure on various polymer surfaces have been seen according to SFG spectra collected as a function of time. On the polyurethane Tecoflex surface, the fibrinogen bend angle increases, indicated by SFG signal decrease (Fig. 8(a)), and the bent molecule gradually changes

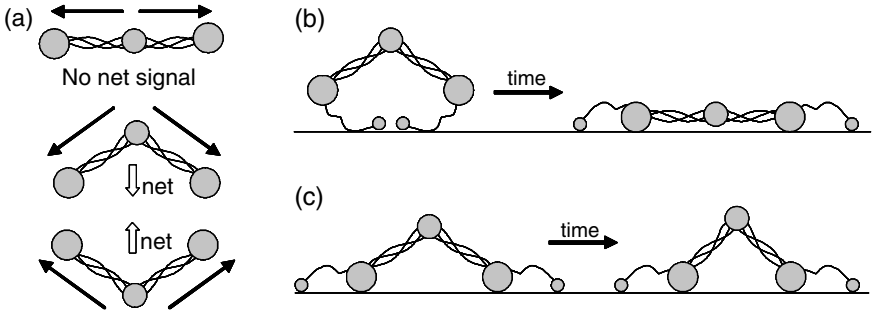

Figure 7. Schematics of varied fibrinogen conformations and conformation changes on different polymer surfaces: (a) linear (top) and bent structures of fibrinogen; (b) fibrinogen structural changes with time after adsorption on Tecoflex; (c) fibrinogen structural changes with time after adsorption on polyurethane–silicone copolymer. (Reproduced with permission from *J Phys Chem B* **109**:22027–22035 (2005). Copyright 2005 American Chemical Society).

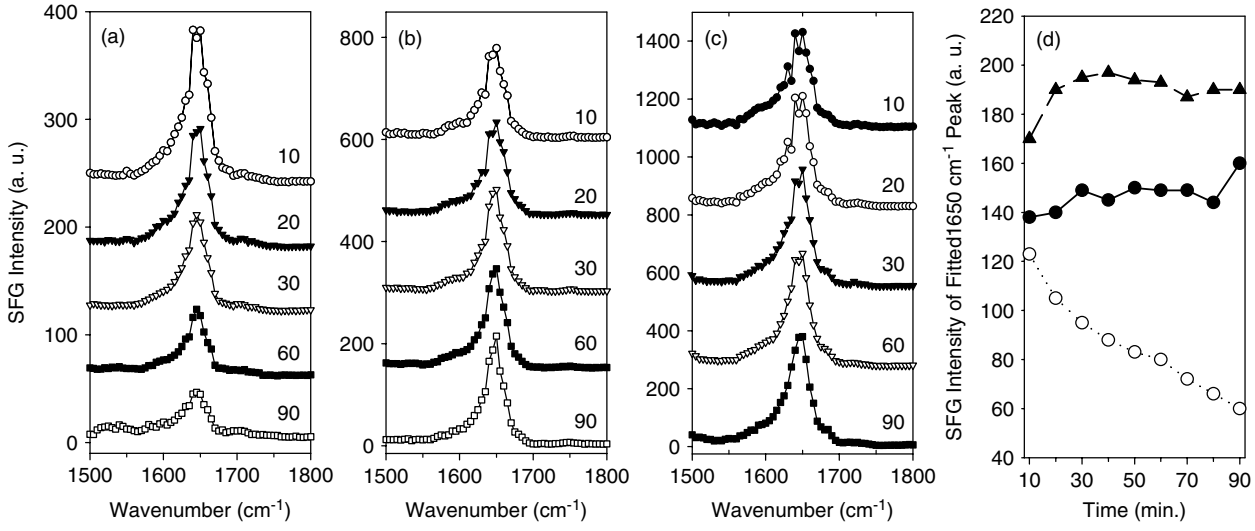

Figure 8. SFG spectra of fibrinogen adsorbed to (a) polyurethane Tecoflex, (b) polyurethane–silicone copolymer carbosil, and (c) fluorinated polymer in PBS buffer in the amide I range collected at different times (in minutes). (d) α-Helix SFG signal as a function of time from fitting SFG spectra for fibrinogen adsorbed to polyurethane Tecoflex (open circles), polyurethane–silicone copolymer carbosil (filled circles) and fluorinated polymer (filled triangles). (Reproduced with permission from *J Phys Chem B* **109**:22027–22035 (2005). Copyright 2005 American Chemical Society).

into a linear structure (Fig. 7(b)) and the SFG signal almost disappears. On the polyurethane–silicone copolymer surface and the fluorinated polymer surface, the bend angle decreases slightly (Fig. 7(c)), resulting in an 'even' bent structure, evidenced by a slight increase of the SFG amide I signal after a period of time (Fig. 8(b) and (c)). On the PS surface, the bend angle increases, but it is much slower compared to the Tecoflex case.[61]

Another important aspect of polymer–protein interactions is that polymer surface structures do respond to protein adsorption. Using SFG, we examined surface structural changes of polymethacrylates after protein adsorption.[63] To avoid spectral confusion, deuterated polymethacrylates were used in the experiments. Using deuterated PEMA and PBMA as examples, according to the peak intensity ratios measured in SFG spectra, we observed that the surface-dominating methyl and methylene groups adopt a structure intermediate to those on the polymer surface in air and in water. This observation is qualitatively similar to those for the buried polymer–polymer interface. It was also detected that adsorption of different proteins on the polymer surface resulted in different orientations of the polymer surface-dominating methyl and methylene groups. These studies indicate that to understand polymer–protein interactions *in situ* it is necessary to study polymer surface structures after protein adsorption.

Adhesives for polymer materials are widely used in almost every area such as the automotive industry, aviation and aerospace, construction, electronics, paints and inks, and beauty and personal care. By understanding adhesion at the molecular level, better adhesives and adhesion promoters for plastics can be developed. Normally it is difficult to examine polymer interfaces with good adhesion *in situ* because such an interface is buried. As shown above, it is feasible to apply SFG to study buried interfaces

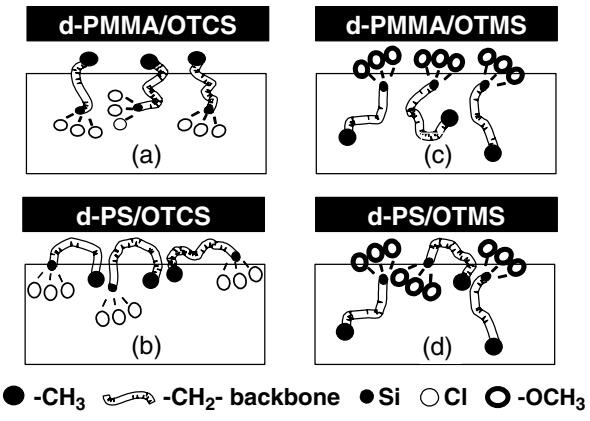

Figure 9. Schematics of different structures of silanes at different polymer interfaces: d-PMMA, deuterated PMMA; d-PS, deuterated PS; OTCS, *n*-octadecyltrichlorosilane; OTMS, *n*-octadecyltrimethoxysilane. (Reproduced with permission from *J Phys Chem B* **107**:10440–10445 (2003). Copyright 2003 American Chemical Society).

involving polymer materials. We used SFG to investigate molecular interactions between various adhesion promoters such as silanes and polymer surfaces.[64–66] We demonstrated that interactions between different silanes and different polymers result in varied interfacial structures of silane molecules at the interfaces: head groups, backbones, end groups, and combinations of such groups can contact the polymer surface depending on the particular interactions between the silane and the polymer (Fig. 9). We also showed that amino silane can diffuse into PMMA, and the diffusion coefficient was determined using SFG to be of the order of $10^{-13}\,cm^2\,s^{-1}$. It was shown that SFG signals from the moving front of the silane during the diffusion can be detected, providing an opportunity to elucidate molecular structures of a moving interface. Hydrogen bonding between an amino silane with another polymer, poly(ethylene terephthalate) (PET), has been observed using SFG. This research shows that different interacting mechanisms between polymer and silane molecules do exist. SFG is a powerful technique to elucidate the molecular mechanisms of polymer adhesion.

CONCLUSIONS

It has been demonstrated that SFG is a powerful tool to probe polymer surfaces and interfaces. In the future, SFG will be an important tool for understanding molecular structures of such surfaces and interfaces not only in academic research, but also in product development and quality control in industry. In addition to academic research laboratories, SFG systems are already available in several companies such as ExxonMobil, Polymer Technology Group, and DuPont. Increasing SFG results for industrial polymer surfaces/interfaces will be generated from industrial researchers and collaborative research between academic and industrial scientists.

To understand the detailed correlation between polymer surface structures and surface properties, it is necessary to generate an extensive database of polymer surface structures using SFG. Surface properties of these polymers should be tested in separate experiments. For example, surface structures of some widely applied biomedical polymers should be carefully studied using SFG, and biocompatibility of these materials will be related to such surface structures. The correlations between surface structures and biocompatibility will serve as standards for designing and developing biomedical polymers with improved surface properties. To understand further why polymer biocompatibility is related to certain surface structural characteristics such as specific surface-dominating groups and their orientation distributions, it is useful to study interactions between several model proteins and polymer surfaces to understand how different surface functional groups with certain orientation distributions mediate protein conformation at the interface. Similar research can be

extended to develop anti-biofouling polymer coatings for marine vessels.

After such an SFG database is generated for polymer surfaces, SFG can be used as an analytical tool for quality control for industrial products with designed surface properties. Also it will be feasible to predict surface properties from surface structures revealed by SFG for new polymers. Since SFG is uniquely sensitive for elucidating buried polymer interfaces, it can be used to elucidate molecular mechanisms of polymer adhesion, and should be able to be developed into a powerful technique to test adhesion of buried interfaces involving polymers.

Conducting polymers are being increasingly used in field effect transistors, light emitting diodes, displays, fuel cells, and solar cells (Gracias D, personal communication). The surface/interface structures of conducting polymers in such devices are considered crucial for the performance of the entire system, and it is necessary to elucidate such surfaces/interfaces *in situ* using SFG. SFG will have broad applications in such studies in the future. Also, polymers are widely used in drug delivery systems. How drug molecules interact with polymer membranes or coatings in such delivery systems should be understood and can be probed using SFG. As mentioned in the introduction, different polymer surfaces can crystallize drug molecules into different polymorphs. Understanding molecular interactions between polymer substrates and drug molecules will provide molecular insight into how to engineer polymer surfaces to optimize polymorphs for drug crystals.

Polymer surface structures with micro- and nano-domains are widely reported. However, to understand the chemical structures of these surface domains is difficult. With the development of SFG microscopy and imaging, it will be feasible to understand such domain structures, designing improved surfaces with micro- or nano-structures for many important applications.

Presently, SFG systems are still not as easy to operate as other vibrational spectroscopic tools such as FTIR and Raman spectroscopy, but commercial SFG systems (e.g. EKSPLA SFG spectrometer) do exist and they do not require extensive adjustment for day-to-day operations. As the development of laser technology and nonlinear optics research continues, SFG systems will be more and more widely used and become easier to handle by non-experts in laser or nonlinear optics. They will contribute more substantially to understanding complicated polymer surfaces/interfaces.

ACKNOWLEDGEMENTS

The author thanks NSF (CHE-0315857, CHE-0449469), ONR (N00014-02-1-0832), Beckman Foundation, and Dow Corning Corporation for the support of this research.

REFERENCES

1 Carbassi F, Morra M and Occhiellp E, *Polymer Surfaces: From Physics to Technology*. John Wiley, Chichester (1994).
2 Feast WJ, Munro HS and Richards RW, *Polymer Surfaces and Interfaces II*. John Wiley, New York (1992).
3 Park JB and Lakes RS, *Biomaterials: An Introduction*. Plenum Press, New York (1992).
4 Wynne KJ and Guard H, *Naval Res* **49**:2 (1997).
5 Lang M, Grzesiak AL and Matzger AJ, *J Am Chem Soc* **124**:14934 (2002).
6 Chen Z, Shen YR and Somorjai GA, *Ann Rev Phys Chem* **53**:437 (2002).
7 Wang J, Clarke ML, Chen X, Even MA, Johnson WC and Chen Z, *Surf Sci* **587**:1 (2005).
8 Chen X, Clarke ML, Wang J and Chen Z, *Int J Mod Phys B* **19**:691 (2005).
9 Loch CL, Ahn D, Chen CY and Chen Z, *J Adhesion* **81**:319 (2005).
10 Shen YR, *The Principle of Nonlinear Optics*. John Wiley, New York (1984).
11 Bain CD, *J Chem Soc Faraday Trans* **91**:1281 (1995).
12 Eisenthal KB, *Chem Rev* **96**:1343 (1996).
13 Scatena LF, Brown MG and Richmond GL, *Science* **292**:908 (2001).
14 Smith JP and Hinson-Smith V, *Anal Chem* **76**:287A (2004).
15 Wang J, Chen CY, Buck SM and Chen Z, *J Phys Chem B* **105**:12118 (2001).
16 Wang J, Woodcock SE, Buck SM, Chen CY and Chen Z, *J Am Chem Soc* **123**:9470 (2001).
17 Wang J, Paszti Z, Even MA and Chen Z, *J Am Chem Soc* **124**:7016 (2002).
18 Chen CY, Wang J and Chen Z, *Langmuir* **20**:10186 (2004).
19 Chen CY, Wang J, Even MA and Chen Z, *Macromolecules* **35**:8093 (2002).
20 Wang J, Even MA, Chen X, Schmaier AH, Waite JH and Chen Z, *J Am Chem Soc* **125**:9914 (2003).
21 Hore DK, Beaman DK and Richmond GL, *J Am Chem Soc* **127**:9356 (2005).
22 Ji N, Ostroverkhov V, Lagugne-Labarthet F and Shen YR, *J Am Chem Soc* **125**:14218 (2003).
23 Zhang D, Shen YR and Somorjai GA, *Chem Phys Lett* **281**:394 (1997).
24 Gracias DH, Zhang D, Lianos L, Ibach W, Shen YR and Somorjai GA, *Chem Phys* **245**:277 (1999).
25 Briggman KA, Stephenson JC, Wallace WE and Richter LJ, *J Phys Chem B* **105**:2785 (2001).
26 Gautam KS, Schwab AD, Dhinojwala A, Zhang D, Dougal SM and Yeganeh MS, *Phys Rev Lett* **85**:3854 (2000).
27 Chen Z, Ward R, Tian Y, Baldelli S, Opdahl A, Shen YR, *et al.*, *J Am Chem Soc* **122**:10615 (2000).
28 Kim D and Shen YR, *Appl Phys Lett* **74**:3314 (1999).
29 Oh-e M, Lvovsky AI, Wei X and Shen YR, *J Chem Phys* **113**:8827 (2000).
30 Zhang D, Gracias DH, Ward R, Gauckler M, Tian Y, Shen YR, *et al.*, *J Phys Chem* **102**:6225 (1998).
31 Chen Z, Ward R, Tian Y, Eppler AA, Shen YR and Somorjai GA, *J Phys Chem B* **103**:2935 (1999).
32 Chen CY, Wang J, Woodcock SE and Chen Z, *Langmuir* **18**:1302 (2002).
33 Opdahl A, Phillips RA and Somorjai GA, *J Phys Chem B* **106**:5212 (2002).
34 Johnson WC, Wang J and Chen Z, *J Phys Chem B* **109**:6280 (2005).
35 Zhang D, Dougal SM and Yeganeh MS, *Langmuir* **16**:4528 (2000).
36 Wei X, Zhuang X, Hong SC, Goto T and Shen YR, *Phys Rev Lett* **16**:4256 (1999).
37 Miyamae T, Yamada Y, Uyama H and Nozoye H, *Appl Surf Sci* **180**:126 (2001).
38 Ye HK, Gu ZY and Gracias DH, *Langmuir* **22**:1863 (2006).
39 Ruckenstein E and Gourisankar SV, *J Colloid Interf Sci* **109**:557 (1986).

40 Lewis KB and Ratner BD, *J Colloid Interf Sci* **159**:77 (1993).
41 Zhang D, Ward RS, Shen YR and Somorjai GA, *J Phys Chem B* **101**:9060 (1997).
42 Chen CY, Clarke ML, Wang J and Chen Z, *Phys Chem Chem Phys* **7**:2357 (2005).
43 Chen Q, Zhang D, Somorjai GA and Bertozzi CR, *J Am Chem Soc* **121**:446 (1999).
44 Li GF, Shen Y, Morita S, Nishida T and Osawa M, *J Am Chem Soc* **126**:12198 (2004).
45 Yang CSC, Wilson PT and Richter LJ, *Macromolecules* **37**:7742 (2004).
46 Gautam KS and Dhinojwala A, *Phys Rev Lett* **88**:145501 (2002).
47 Wilson PT, Briggman KA, Wallace WE, Stephenson JC and Richter LJ, *Appl Phys Lett* **80**:3084 (2002).
48 Wilson PT, Richter LJ, Wallace WE, Briggman KA and Stephenson JC, *Chem Phys Lett* **363**:161 (2002).
49 Kweskin SJ, Komvopoulos K and Somorjai GA, *Langmuir* **21**:3647 (2005).
50 Ye S, Morita S, Li GF, Noda H, Tanaka M, Uosaki K, *et al.*, *Macromolecules* **36**:5694 (2003).
51 Chen CY, Even MA, Wang J and Chen Z, *Macromolecules* **35**:9130 (2002).
52 Chen CY, Even MA and Chen Z, *Macromolecules* **36**:4478 (2003).
53 Kim G, Gurau M, Kim J and Cremer PS, *Langmuir* **18**:2807 (2002).
54 Jung SY, Lim SM, Albertorio F, Kim G, Gurau MC, Yang RD, *et al.*, *J Am Chem Soc* **125**:12782 (2003).
55 Kim J and Somorjai GA, *J Am Chem Soc* **125**:3150 (2003).
56 Wang J, Buck SM, Even MA and Chen Z, *J Am Chem Soc* **124**:13302 (2002).
57 Sartenaer Y, Humbert C, Mani AA, Methivier C, Pradier CM, Thiry PA, *et al.*, *Chem Phys Chem* **5**:1719 (2004).
58 Wang J, Chen XY, Clarke ML and Chen Z, *Proc Natl Acad Sci USA* **102**:4978 (2005).
59 Chen XY, Wang J, Sniadecki JJ, Even MA and Chen Z, *Langmuir* **21**:2662 (2005).
60 Clarke ML, Wang J and Chen Z, *J Phys Chem B* **109**:22027 (2005).
61 Wang J, Chen XY, Clarke ML and Chen Z, *J Phys Chem B* **110**:5017 (2006).
62 Knoesen A, Pakalnis S, Wang M, Wise WD, Lee N and Frank CW, *IEEE J Sel Top Quantum Electron* **10**:1154 (2004).
63 Clarke ML and Chen Z, *Langmuir* **22**:8627 (2006).
64 Chen CY, Loch CL, Wang J and Chen Z, *J Phys Chem B* **107**:10440 (2003).
65 Chen CY, Wang J, Loch CL, Ahn D and Chen Z, *J Am Chem Soc* **126**:1174 (2004).
66 Loch CL, Ahn D, Wang J, Chen CY and Chen Z, *Langmuir* **20**:5467 (2004).